Carbapenem heteroresistance of KPC-producing *Klebsiella pneumoniae* results from tolerance, persistence and resistance.

[1,2,3,4]Adriana Chiarelli, [1,2,4]Nicolas Cabanel, [1,2,4]Isabelle Rosinski-Chupin, [4,5,6]Thomas Obadia, [7]Raymond Ruimy, [1,9]Thierry Naas, [1,9]Rémy A. Bonnin, [1,2,4]Philippe Glaser*

[1]Evolution and Ecology of Antibiotic Resistance Unit, Institut Pasteur-APHP-University Paris-Saclay. [2]CNRS UMR6047, 75015, Paris, France. [3]Sorbonne Université, Paris, France. [4]Université Paris Cité, Paris, France. [5]Institut Pasteur, Infectious Disease Epidemiology and Analytics G5 Unit, F-75015, Paris, France. [6]Institut Pasteur, Bioinformatics and Biostatistics Hub, F-75015, Paris, France. [7]Department of Bacteriology, Nice Academic Hospital, Nice, France. [8]Université Côte d'Azur, and Inserm, C3M, Nice, France Nice, France. [9]UMR1184 Team RESIST, Faculty of Medicine University Paris-Sud, University Paris-Saclay, French National Reference Center for Antibiotic Resistance: Carbapenemase producing Enterobacteriaceae, Le Kremlin-Bicêtre, France.

* Corresponding author: Philippe GLASER,
Institut Pasteur, 28 Rue du Dr Roux, 75724 Paris Cedex 15, Tel + 33 1 45 68 89 96 –
E-mail: pglaser@pasteur.fr

Short title: Carbapenem heteroresistance of KPC-producing Klebsiella pneumoniae

ABSTRACT

Carbapenemase-producing *Klebsiella pneumoniae* (CPKp) have disseminated globally and represent a major threat in hospitals with few therapeutic options and high mortality rates. Isolates producing the carbapenemase KPC (KPC-Kp) might be classified as susceptible according to clinical breakpoints by antibiotic susceptibility testing (AST), allowing the use of imipenem or meropenem for treatment of infections. However, some KPC-Kp show heteroresistance (HR) to carbapenems, with colonies growing in the inhibition halo of agar-based AST. HR KPC-Kp have been associated with a higher risk of treatment failure. Here, we characterized the diversity of mechanisms behind HR to imipenem of these isolates. By analyzing a diverse collection of CPKp, we showed that HR is frequent among KPC-Kp. By monitoring single HR colony appearance using the ScanLag setup, we discriminated surviving cells in two subpopulations leading to a Gaussian-like distribution of early-appearing colonies, with a delayed emergence compared to colonies arising in the absence of antibiotics, and a long tail of late-appearing colonies. A subset of colonies showed a reduced growth rate. Characterization of surviving populations by AST and whole-genome sequencing of 333 colonies revealed a majority of parental genotypes and a broad landscape of genetic alterations in 28% of the colonies, including gene loss, DNA amplification and point mutations. This unveils the complexity of imipenem HR among KPC-Kp isolates, which involves tolerant and persistent cells, but also resistant bacteria. These observations contribute to a better understanding of reasons behind carbapenem treatment failure of KPC-Kp isolates.

AUTHOR SUMMARY

In the course of an antibiotic treatment, bacteria will encounter varying drug concentrations with different potential for their elimination and resistance selection. The ability of a bacterium to defeat antibiotics not only depends upon resistance, but also on tolerance and persistence, which allow a bacterial population to temporarily survive high drug doses. Carbapenems are antibiotics of last resort and *Klebsiella pneumoniae* isolates producing the carbapenemase KPC are a threat to hospitals, although they might remain susceptible to carbapenems. However, seemingly homogeneous populations of KPC-*K. pneumoniae* isolates frequently show varying degrees of susceptibility to carbapenem, i.e., a phenomenon called heteroresistance. We characterized bacteria surviving a high dose of imipenem, progressively degraded by the released carbapenemase, by monitoring the growth of the resulting colonies using the ScanLag system, their genome sequence and carbapenem susceptibility. We show that the observed phenotypic diversity combines tolerance, persistence and resistance making the treatment with high doses of carbapenems frequently inefficient.

64 **INTRODUCTION**

65 Antibiotic resistance represents a global health concern. Several bacterial pathogens evolved
66 multi-drug resistance (MDR), critically affecting their clinical management. Carbapenem-
67 resistant Enterobacterales (CRE), including *Klebsiella pneumoniae*, were listed by the World
68 Health Organization as critical priority pathogens for which there is an urgent need to develop
69 new antibiotics [1]. Carbapenem resistance may arise from the production of an extended-
70 spectrum ß-lactamase (ESBL) or a cephalosporinase associated with decreased permeability
71 due to mutations in porin genes and/or upregulation of efflux pumps, or resulting from the
72 production of specific carbapenem-hydrolysing β-lactamases (carbapenemases) [2].
73 Carbapenemase-producing *K. pneumoniae* (CPKp) is one of the most feared nosocomial
74 pathogen worldwide [3]. Carbapenemases belong to Ambler class A (KPC-type), class B
75 (metallo-β-lactamases IMP, VIM- and NDM-types) or class D (OXA-48-like enzymes) of ß-
76 lactamases [4] with variable occurrence according to geographical areas [5, 6]. In clinical
77 practice, CPKp may be treated with high doses of carbapenem depending on the minimum
78 inhibitory concentration (MIC) [7]. Indeed, production of a carbapenemase leads to a decreased
79 susceptibility to carbapenems but can remain under clinical breakpoints. However, treatment
80 effectiveness is extremely dependent on the accurate measurement of carbapenem MIC [8], and
81 MIC determination is often challenged by variable resistance levels shown by CPKp, especially
82 those producing the class A carbapenemase KPC (KPC-Kp) [9, 10].

83 A further challenge is represented by heteroresistance (HR) towards carbapenems. Antibiotic
84 HR broadly describes heterogeneous susceptibility levels to an antibiotic within seemingly
85 isogenic bacterial populations. This "bet-hedging" survival strategy confers long-term fitness
86 benefit to populations in constantly fluctuating environments [11]. In addition, as resistance is
87 often a stepwise evolutionary process, such heterogeneity may precede genetic changes, and
88 accelerate resistance development in the population [12, 13]. Antibiotic HR itself corresponds
89 to different situations according to the clonality of resistant subpopulations compared to the
90 bulk of the population, the resistance level and the stability of the observed phenotype [14].
91 Most of the studies addressing the HR issue adopt the Population Analysis Profiling (PAP)
92 method, although following different parameters. Yet, there is a general consensus that a strain
93 can be defined as HR when showing subpopulations growing at more than eight times the MIC
94 of the main cell population [14].

95 Antibiotic HR has been largely reported among *K. pneumoniae* isolates towards colistin and
96 corresponding to resistant subpopulation due to mutations modifying the LPS charge [15, 16].
97 Although to a minor extent, HR has also been described towards carbapenems [17-20].

98 Carbapenems HR was mostly observed among KPC-Kp [19-21]. However, mechanisms
99 mediating carbapenem HR in *K. pneumoniae* remain poorly characterized. Heteroresistant
100 KPC-Kp strains survival upon exposure to high bactericidal concentrations of imipenem (IMP)
101 was shown to result from the emergence of a resistant mutated subpopulations with decreased
102 expression of the major outer membrane porin (OMP), OmpK36 [21, 22]. Survival is likely
103 favored in the first place by IMP degradation driven by KPC released into the culture medium,
104 reminding of the phenomenon of indirect resistance, where an antibiotic resistant bacteria
105 contribute to the growth of susceptible ones [23].
106 Here, we aimed at characterizing carbapenem HR in KPC-Kp clinical isolates and identifying
107 metabolic and regulatory pathways underlying the diversity of susceptibility levels to high
108 doses of carbapenems. We characterized phenotypically and genotypically a collection of 62
109 KPC-Kp isolates, in addition to 20 *K. pneumoniae* isolates producing other carbapenemases. A
110 subset of KPC-Kp isolates was further selected to infer the dynamics of bacterial response to
111 high doses of IMP at single colony level [24]. Through the characterization of surviving
112 subpopulations, we showed that HR to imipenem in KPC-Kp is a multifaceted phenomenon,
113 which encompasses different mechanisms adopted by bacterial populations to survive drug
114 exposure, namely tolerance, persistence and resistance. This approach also revealed a broad
115 diversity of genetic alterations in diverse pathways associated with the observed phenotypes.
116
117
118 **RESULTS**
119
120 **Diversity of carbapenem resistance and prevalence of heteroresistance among KPC-Kp.**
121 In order to characterize HR among KPC-Kp, we collected 62 KPC-Kp clinical isolates. For
122 comparison, we included 20 clinical isolates expressing other carbapenemases and three clinical
123 isolates without any carbapenemase as control (S1 Table). Whole genome sequence (WGS)
124 analysis revealed that the KPC-Kp isolates belong to 16 STs, with ST512 being the most
125 prevalent (n = 19), followed by ST101 (n = 10) and ST258 (n = 8). Thirteen different capsular
126 types were identified, with KL107 being the most represented one (n = 24) and mostly
127 associated with ST512. In addition to the carbapenemase genes, the 82 CPKp isolates displayed
128 diverse antibiotic resistance genes and porin mutations (S1 Table). Defects in at least one of the
129 major porin genes (*ompK35* and *ompK36*) were detected in 66% of isolates (n = 54/82) and,
130 among them, 33% (n = 18/54) co-harbored an ESBL gene. In agreement with previous studies,

131 CPKp ST512 isolates shared a truncated *ompK35* sequence and a G134D135 duplication in the
132 sequence of the OmpK36 L3-loop, resulting in a narrower pore and yielding similar resistance
133 levels as a porin inactivation [25]. Likewise, CPKp ST258 isolates exhibited a truncated
134 *ompK35* sequence and, two of them had the same *ompK36* GD duplication. The ten ST101
135 CPKp isolates shared a frameshift mutation in *ompK35* and nine of them also had a TD or GD
136 duplication in *ompK36* and one a D duplication in OmpK36 L3-loop (S1 Table).
137 The susceptibility levels to IMP and MEM were determined by Etest strip, as the broth
138 microdilution method might be affected by carbapenem degradation [26]. The carbapenemase-
139 producing isolates exhibited a broad range of MICs, from 0.125 to >32 mg/L to MEM and 0.25
140 to >32 mg/L to IMP respectively (S1 Table). All the IMP R isolates (n = 19) exhibited defects
141 in the sequence of at least one major porin, with 95% (n=18/19) showing altered sequences of
142 both *ompK35* and *ompK36*. All MEM R isolates (n = 38) but one showed at least one mutation
143 in *ompK35*, with 89% having both *omp* genes disrupted (n = 34). A minority of MEM R isolates
144 (9/38) and IMP R isolates (5/19) carried at least one ESBL gene. This observation suggested
145 that higher carbapenem MICs did not result of the expression of an ESBL in the KPC-Kp
146 isolates we have analyzed but mainly of reduced OM permeability.
147 We next evaluated HR of these isolates based on the appearance of colonies within the
148 inhibition halo induced by the Etest antibiotic gradient strip (Fig 1A). Isolates showing full
149 contact with the Etest gradient strip (IMP, n = 3; MEM, n = 31) for which HR could not be
150 detected were excluded from the analysis (Fig 1A). According to the criteria defined in the
151 Methods section, 73% (n = 43/59) and 51% (n = 17/31) of the KPC-Kp isolates were identified
152 by Etest as HR or moderate HR to IMP and MEM, respectively (Fig 1B, S1 Table). A higher
153 rate of IMP HR was detected for isolates otherwise classified as susceptible (78%) or
154 intermediate (80%) based on their MIC compared to resistant ones (67%). In the case of MEM,
155 HR was more frequent with isolates classified as intermediate (58%) (Fig 1B). In addition, 71%
156 of isolates carrying $bla_{\text{KPC-2}}$ showed MEM HR isolates, in contrast with only 30% of those
157 harboring $bla_{\text{KPC-3}}$ (Fig 1C). Using the same criteria, HR was also detected by Etest among
158 NDM-producing *K. pneumoniae* (n = 3/5 HR to IMP 2/5 HR to MEM), but was not observed
159 among the VIM- and OXA- and control isolates (S1 Table).
160 Altogether, these results showed that our set of isolates harboring bla_{KPC} exhibited a broad
161 range of resistance and HR levels.
162
163 **KPC-Kp isolates show subpopulations growing at high imipenem doses.** Based on MIC
164 values and HR data, we selected seven KPC-Kp in our set of isolates to characterize their

165 response to IMP concentrations 4-, 8- and 10-fold their MICs, as determined by Etest. For
166 comparison, two NDM-Kp, two OXA-Kp and two VIM-Kp were also analyzed (in bold in S1
167 Table). To evaluate the impact of the growth phase on the survival of subpopulations to IMP,
168 bacterial cultures in exponential (EP) and stationary phase (SP) were tested.
169 According to the definition of HR, isolates showing colonies at least at IMP 8xMIC were
170 considered as heteroresistant. We detected HR, to varying degrees, in four KPC-Kp isolates:
171 CNR146C9, CNR121E10, KP H15-21-6 and BIC-1 (Fig 2A). The highest frequency of survival
172 at 8- and 10-fold MIC of IMP was observed for CNR121E10, followed by CNR146C9, thus
173 confirming their HR profile displayed by Etest. Interestingly, KP H15-21-6 was not HR by
174 Etest, but showed surviving subpopulations by PAP. On the other hand, although NDM isolates
175 showed a HR-like pattern by Etest, they did not show HR by PAP assay at 8-fold MIC of IMP.
176 VIM- and OXA-isolates showed scarce or none ability to grow at 8-fold MIC IMP, in
177 agreement with undetected HR profiles by Etest. Significant differences between EP and SP
178 inoculum were observed for four out of the 13 isolates at 8-fold MIC (Fig 2B). The two KPC-
179 Kp (CNR146C9 and CNR121E10) and the VIM-Kp (CNR206A5) isolates showed a higher
180 frequency of surviving subpopulations in SP, suggesting a persister-like subpopulation.
181 However, the KP1 strain, producing VIM-1, displayed a higher number of surviving CFUs in
182 EP than in SP. These observations suggested a strain-specific ability to cope differently with
183 high doses of IMP, according to the physiological state of the bacterial population.
184
185 **Subpopulation growth dynamics**. Differences in colony size were noticed on medium
186 supplemented with 8-fold MIC IMP for CNR146C9, CNR121E10, Kp H15-21-6 and BIC-1
187 (S1A Fig.), indicating an heterogeneous growth of surviving subpopulations in the presence of
188 IMP. To better characterize the dynamics by which subpopulations survive exposure to high
189 IMP concentrations, we tracked appearance and growth of individual colonies in the presence
190 of IMP by ScanLag [24]. For comparison, we included in our analysis two KPC-Kp isolates
191 showing scarce or none HR (CNR149B2 and CNR152H4). For these two isolates, colony
192 behavior was investigated at 4xMIC IMP, as the number of CFUs at 8xMIC was below our
193 detection threshold (less or equal than 10^2 CFU/ml). Imipenem MICs for the six selected KPC-
194 Kp isolates ranged from 0.25 to 1.5 mg/L (S1 Table).
195 By using ScanLag, we quantified the distribution of colony time of appearance (ToA) of the six
196 isolates over 48 hours onto drug-free and IMP-containing media (Fig 3A). In the absence of
197 IMP, we observed a narrow normal distribution of ToA for all the isolates, with mean values
198 ranging from 426 to 518 minutes (S2 Table, Fig 3A; cyan blue bars). By contrast, the

199 distribution of colony ToA onto media supplemented with IMP was heterogeneous with a main
200 peak and a tail of varying length, particularly visible in CNR146C9, CNR152H4 and
201 CNR121E10 (Fig 3A, red bars).
202 The bimodal distribution suggested for the six strains the existence of two subpopulations: an
203 early appearing N1 population corresponding to the main peak of ToA, and a late-appearing
204 N2 population indicated by the tail. To characterize the observed heterogeneity, we attempted
205 to fit the data to a two-component mixed model using ToA as index. This approach allowed us
206 to quantify the proportions of the N1 and N2 subpopulations across the six isolates and the
207 heterogeneous delay in growth (here referred to as lag time extension, LE) of the N1 population
208 relative to the colonies appearing on drug-free media (Fig 3B, Table S2). To estimate the
209 influence of the bacterial growth phase on the survival rate and on the frequency of
210 subpopulations N1 and N2, we also tracked the colony ToA upon spreading stationary phase
211 (SP) cultures of the six isolates on the drug-free and IMP-supplemented agar media.
212 N1 subpopulation from isolates CNR149B2, Kp H15-21-6 and BIC-1 grown up to EP showed
213 an earlier appearance (LE <2) in comparison with the other three isolates, with LE ≥ 2 (Fig 3C,
214 green boxplots). Since SP cultures have been shown to be more tolerant to ß-lactams [27], we
215 expected to observe an extended delay in growth for SP cultures exposed to IMP. However, by
216 quantifying the LE of N1 subpopulations, we could detect a significantly longer delay only for
217 CNR149B2 and Kp H15-21-6 in SP compared to EP (Fig. 3C).
218 As previously proposed [28], colonies that appeared later than three standard deviations away
219 from the mean of the main peak distribution (subpopulation N1) were hypothesized as
220 derivative of persister cells, restoring growth only upon gradual exhaustion of IMP below the
221 MIC. We estimated their frequency for the six isolates after plating on 8-fold MIC IMP (4-fold
222 for strains CNR133C4 and CNR152H4) from exponential or stationary phase cultures. The
223 highest frequency of persisters in exponential phase was observed for CNR146C9, whereas
224 BIC-1 exhibited the lowest frequency (Fig 3D). We did not detect any significant difference in
225 the proportions of persisters between the EP and SP, except for CNR146C9 (p-value = 0.0038),
226 which surprisingly showed a lower occurrence of persisters in SP, in contrast with the increased
227 survival of SP grown bacteria as observed by PAP (Fig 3D, S2 Table).
228 Overall, we observed heterogeneous growth resumption among the selected isolates when
229 plated on high concentrations of IMP (4-fold MIC or 8-fold MIC), which suggested the co-
230 existence of at least two distinct phenotypes in the surviving populations. Both the growth delay
231 (measured as lag time extension) and the proportion of the subpopulations N1 and N2 were
232 strain-specific, likely linked to differences in the genomic backgrounds of the isolates.

233

234 **Genetic heterogeneity associated with the observed heteroresistance**. Antibiotics HR refers
235 to a phenotypically heterogeneous subpopulation within a seemingly isogenic population.
236 However, increased survival might be also linked to genetic alterations. We selected
237 CNR146C9 for in-depth genetic analysis of the HR populations and to better discriminate the
238 events responsible for enhanced survival. To obtain a high quality reference genome, we
239 determined its whole genome sequence by combining long- and short-read sequencing.
240 CNR146C9 hosts two plasmids carrying $bla_{\text{CTX-M-15}}$ and $bla_{\text{KPC-3}}$ of 237,007 bp and 110,489 bp,
241 respectively and a circular 52,608 bp-long extrachromosomal phage, previously reported in
242 *K. pneumoniae* ST307 isolates [29] (S3 Table).
243 Based on the ToA and colony growth rates as visualized by ScanLag (Fig 3A), we classified
244 surviving colonies according to three patterns: A, B and C (S1B Fig). Patterns A and B emerged
245 before the cut-off for persisters (on average 1382 min) and globally correspond to the
246 subpopulation N1. Pattern A included colonies showing wild-type or near wild-type growth
247 rates, whereas pattern B corresponded to colonies with reduced growth rates, as observed by
248 ScanLag. Pattern C colonies emerged after the cut-off for persisters, showing a wild-type
249 growth rate but delayed and variable ToA. They corresponded to the N2 subpopulation, the tail
250 of the ToA distribution. A total of 333 colonies (167 of pattern A, 30 of pattern B and 136 of
251 pattern C) were submitted right after isolation and 2 hour-growth in LB broth to WGS and IMP
252 and MEM MIC determination by Etest. Ninety-four colonies showed at least one genetic
253 modification, including single-nucleotide variations (SNVs), insertions, deletions of bases,
254 plasmid/phage loss and amplification (Fig 4A) affecting a broad range of functions (Fig 4B).
255

256 **Pattern A colonies result from tolerance or resistance to IMP.** For most of the A-type
257 colonies (128/167), we did not detect any genetic change. These colonies exhibited MIC values
258 for MEM and IMP and an HR profile determined by Etest similar to the parental strain
259 CNR146C9, suggesting they have survived in the presence of IMP until it reaches a
260 concentration lower than the MIC. Thirty-nine A-isolates showed genetic alterations (S4
261 Table). Most of them were not associated with a decreased susceptibility to both carbapenems
262 (63%). The most recurrent event was the loss of the 52,608 bp extrachromosomal phage (n=12).
263 One ICE and part of the *tra* region from the CTX-M-15 plasmid (n=3) were also lost. Point
264 mutations were also detected among those colonies and affecting different functions like a
265 nonsense mutation in *lysS* encoding one of the two tRNA synthase gene or a mutation in *rpsC*
266 encoding the ribosomal protein S3. Some of these diverse genetic events might have been

267 selected and contributed to longer IMP survival. On the other hand, 15 colonies showed a
268 decreased susceptibility to IMP and MEM ranging from 1.5 mg/L to >32 mg/L. Strikingly, all
269 mutations detected in these colonies except one were associated with alterations of the cell
270 envelope. Mutations leading to the highest MICs affected the OM permeability, with three
271 clones mutated in *ompK36*. However, non-canonical mutations affecting the Bam pathway of
272 insertion of OMP into the outer membrane OM [30] were also selected. Three clones showed a
273 truncated *bamB* gene, one was mutated in *bamA* (N448Y), which is essential, and one isolate
274 showed an IS*Kpn25* insertion six bp upstream of the start codon of the *surA* gene encoding the
275 major chaperon molecule contributing to the translocation of OMP across the periplasm [31].
276 In addition, three clones show mutations affecting LPS biosynthesis and three others mutations
277 in regulatory systems affecting cell wall components. Among these last isolates, AC90-A
278 carried two mutations in the *cpxAR* locus encoding a two component regulatory system sensing
279 OM stresses [32, 33]: a four codons deletion (pos. 20 to 23) in the sensor *cpxA*, present in 100%
280 of the reads and a R205W mutation in *cpxR* present in 95% of the reads. This clone is
281 heterogeneous with dominant large colonies, mutated in *cpxR* and *cpxA* showing WT MICs to
282 IMP and MEM and few highly resistant small colonies, only mutated in *cpxA* (S4 Table). The
283 only mutation associated with reduced susceptibility but not affecting the cell envelope
284 occurred in the *lipA* gene, involved in lipoyl cofactor biosynthesis. Lipoyl is a cofactor of
285 pyruvate and 2-ketoglutarate dehydrogenases, key enzymes of glycolysis and the tricarboxylic
286 acid (TCA) cycle. This metabolic mutation reminds the type of mutations from the B pattern
287 (see below).
288 Heteroresistance has been shown to result frequently from gene amplification leading to an
289 increased gene expression [34]. We systematically searched for DNA amplifications in the 333
290 genomes. We identified three cases of genome amplification among the A-type isolates (S4
291 Table). In strain AC376, we observed a 89,584 bp ectopic duplication encompassing the *dcw*
292 locus encoding major functions for cell wall synthesis and cell division, the additional copy
293 being inserted upstream the transcriptional regulatory gene *qseB* (Fig. 5A). Interestingly, this
294 isolate showed a 16-fold decreased IMP susceptibility but almost no effect on MEM
295 susceptibility.
296 Strain AC150-A showed a c.a. 68 kb-long duplication within the pKPC plasmid and
297 encompassing $bla_{\text{KPC-3}}$ (Fig. 5B). This duplication might be responsible for a doubling of the
298 MICs for IMP and MEM of this strain. On the other hand, the gene coverage of pKPC was
299 variable across all isolates with an average normalized coverage ranging from 0.39 to 2.62
300 excluding isolates which have lost pKPC. The 11 isolates with the highest pKPC coverage

301 (ranging from 1.88 to 2.62-folds higher than the average) all belong to the A class. However,
302 except AC150-A, none showed an increased MIC to IMP and MEM as quantified by E-test.
303
304 **Colonies of B-pattern are mainly small colony variants** Twenty-two out of the 30 B-pattern
305 colonies here analyzed showed an increased MIC for both carbapenems. The eight remaining
306 isolates might have been misclassified as pattern B or the phenotype was highly unstable, as
307 after re-isolation they did not phenotypically differentiate from the parental strains (S5 Table).
308 We identified mutations in 28/30 isolates (Table S5) and 67% occurred in genes with metabolic
309 functions. The most recurrent mutations affected respiration with mutations found in the
310 coenzyme Q synthesis genes *ubiA* (n=2), *ubiB* (n=2), *ubiD* and *ispA* (n=3), in the heme
311 biosynthesic gene *hemA* and in genes involved in the TCA cycle (a deletion encompassing *lpdA*
312 and *aceF*; *icd*, encoding isocitrate dehydrogenase (n=2) and *acnB*, encoding the aconitate
313 hydratase (n=2)). One isolate showed inactivation of the gene *ptsI* from the central
314 phosphotransferase system (PTS), contributing to carbon source import and catabolic
315 regulation in *E. coli* [35]. In the presence of oxygen, these mutants showed tiny colonies with
316 fastidious growth, which are features of small colony variant (SCV) [36]. Under these
317 conditions, they also showed an increased resistance to IMP and MEM. However, under
318 anaerobiosis, these phenotypic traits were reversed for respiratory and TCA mutants. Therefore
319 the metabolic defect was likely responsible for the phenotype (S5 Table). Two mutations
320 affected lipid metabolism: *pgpC* encoding a phosphatidylglycerophosphatase C and *hldE,*
321 encoding a bifunctional kinase/adenylyltransferase involved in the inner core LPS biosynthesis
322 [37]. One isolate mutated in *cysB* showed an increased MICs only towards IMP. Interestingly,
323 *cysB* mutation is the major cause of mecillinam resistance in clinical isolates of *E. coli* [38].
324 One isolate (AC171-B) mutated in the $tRNA^{Ser}$(gct) encoding gene showed a moderate decrease
325 in susceptibility to both carbapenems and a strong growth defect, possibly due to altered protein
326 synthesis. Globally, pattern B corresponded to resistant bacteria with mutations in
327 *K. pneumoniae* core resistome and associated with decreased growth rate, as observed by
328 ScanLag.
329
330 **Pattern C colonies likely correspond to persisters.** Unlike colonies from pattern A and B,
331 none of the pattern C colonies showed a significant increase in the MICs to carbapenems and
332 86% (n=117/136) did not show any detectable genetic modification. Unexpectedly, ten colonies
333 showed an increased susceptibility to the two carbapenems due to the loss of the pKPC plasmid
334 (S6 Table). As observed for pattern A colonies, four patterns C colonies showed loss of the

335 phage, whereas one clone (AC158-C) lost an integrated prophage. In one isolate (AC362-C),
336 we observed a 3-fold copy number increase of a 51 kb long region from the pCTX-M plasmid
337 bracketed by two IS*5075* (S2 Fig). This genomic island contains numerous adaptive functions
338 for glycogen biosynthesis, lactose catabolism, the Fe(3+) dicitrate transport system (*fec* locus)
339 and a glutathione transport system [29]. Increased expression of these genes might have
340 contributed to the enhanced survival as persistent cell. Two colonies showed intergenic
341 mutations, while one nonsense mutation inactivates the type VI secretion system protein TssG.
342 Whether these mutations contribute to the persistent phenotype remain to be determined.
343 The late appearance of the colonies and the nature of the seldom genetic events observed that
344 are not contributing to ß-lactam resistance are in agreement with colonies resulting from
345 persistent cells. These bacteria escaped the imipenem bactericidal effect until its concentration
346 became lower than CNRR146C9 IMP MIC (0.5 mg/L) or until it is even below the MIC of a
347 strain devoid of $bla_{\text{KPC-3}}$ (0.19 mg/L).
348
349 **DISCUSSION**
350 Although the expression of the KPC carbapenemase confers reduced susceptibility to
351 carbapenems, MICs for imipenem are frequently below the breakpoint for susceptibility (1
352 mg/L, EUCAST), as we have observed in the set of 62 KPC-Kp clinical isolates analyzed in
353 this work. Such MICs are theoretically compatible with the usage of IMP to treat those isolates,
354 but with an increased risk of resistance selection and treatment escape [7]. Moreover,
355 occurrence of HR to IMP may further complicate the management of KPC-Kp isolates in
356 clinical practice.
357 In addition to variable MICs, the KPC isolates here analyzed showed different levels of HR
358 towards IMP and MEM. The proportion of isolates showing HR to IMP was higher than those
359 with an HR profile to MEM. These two carbapenems share similar mode of action by targeting
360 mainly PBP2, but also binding to PBP1a PBP1b. In addition, MEM shows a higher affinity to
361 PBP3 [39], explaining differences in the morphological impact of those two carbapenems on
362 *E. coli* cells [40]. On the other hand, IMP is a smaller molecule than MEM and shows a rapid
363 influx through the OM [41]. More importantly, under laboratory conditions, IMP is less stable
364 than MEM and is spontaneously degraded [41, 42], likely contributing to the higher rate of HR
365 towards IMP comparted to MEM. We observed a higher proportion of HR towards MEM of
366 isolates expressing KPC-2 compared to those expressing KPC-3 (Fig 1C), which might be
367 linked to a higher stability (longer half-life) of KPC-2 [43] contributing to a extended
368 degradation of MEM in the solid medium.

369

370 HR has been defined as the occurrence of a bacterial subpopulation surviving treatment at 8x
371 the MIC of the drug [14]. In our PAP analyses, at this antibiotic concentration, frequency of
372 survival ranged from 5.3 x 10^{-6} to 4.76 x 10^{-4}. This low frequency challenges the harvest of the
373 surviving population, limiting the use of microscopy for single cell analysis on agarose-pad or
374 microfluidics device such as the mother machine [44]. Previous studies addressing HR in KPC-
375 Kp were performed in bulk, following addition of IMP at concentrations higher than the MIC
376 leading to the selection of resistant mutants in the porin gene *ompK36* [21, 22]. Here, we applied
377 the ScanLag system [24] to analyze the individual fate of surviving bacteria forming colonies
378 on media supplemented with IMP at 8xMIC or 4xMIC. For the six KPC-Kp isolates analyzed,
379 ScanLag revealed a bimodal profile of colony appearance in the presence of IMP: a Gaussian
380 peak, delayed compared to the peak of appearance of the colonies not exposed to IMP, followed
381 by a tail of late appearing colonies. In addition to the delayed time of appearance, some colonies
382 showed a slower growth rate. Compared to other antibiotics, a specific parameter of HR to ß-
383 lactams in ß-lactamase producing bacteria is the degradation of the antibiotic in the medium.
384 The first Gaussian peak of the surviving populations N1 is consistent with what has been
385 defined as tolerant by adjusting lag time [45]. Similarly, the late appearing colonies (N2) in the
386 tail of the distribution, emerging under conditions where the antibiotic is gradually degraded
387 would result from persister cells [28, 45]. In agreement with these hypotheses, the vast majority
388 of colonies from N1 and N2 populations of strain CNR146C9 reproduced the same
389 susceptibility and HR phenotype as the parental strain. Comparisons of the six clinical isolates
390 showed different profiles and effects of plating EP or SP bacteria (Fig. 3B and D), reflecting
391 different levels of tolerance and persistence towards IMP. Such differences in drug survival are
392 likely due to the genomic context, which remains to be fully investigated. As characterized in
393 experimental models of evolution [46, 47], these features might have been selected in synergy
394 with the selection of antibiotic resistance following drug treatments in the host.
395 One limitation of ScanLag is the absence of information on the first generations before the
396 appearance of a visible colony. The observed delay might be related to an extended lag phase
397 or to a transient slow growth phase reducing susceptibility. We speculated that combining
398 genomic and phenotypic analyses of surviving colonies at 8xMIC would provide additional
399 information on surviving populations. Most of the clones from profile A and C (from N1 and
400 N2 populations respectively) showed a phenotype similar to the parental strain and did not
401 exhibit any genetic events, which is in agreement with tolerance and persistence mechanisms,
402 respectively. The frequent loss of pKPC plasmid in ten of the C-isolates was intriguing. Indeed,

403 no plasmid loss was detected among 196 colonies of the parental strain CNR146C9 growing
404 on antibiotic-free medium. The pKPC carries functions contributing to its stability including a
405 *vapBC* family toxin/antitoxin (TA) locus. VapC toxins inhibit translation by an RNAse activity
406 [48]. In *E. coli*, the VapBC TA system was previously reported to contribute to increased rate
407 of persistence [49] and a *vapB* mutant was associated with an extension of lag-time and higher
408 drug tolerance in *E. coli* exposed to intermittent high doses of ampicillin [45]. We hypothesized
409 that the loss of pKPC might lead to a transient activation of VapC resulting of the instability of
410 VapB and a growth arrest contributing to the persistent state. Therefore, pKPC loss would be
411 under positive selection in the set-up we have used, supporting the hypothesis that C-type
412 colonies arose mainly from persisters. Interestingly, loss of the KPC-plasmid was previously
413 observed in clinical KPC-Kp isolates [50]. In this context, the host response or antibiotic
414 treatments might have contributed to a similar selection of persister cells. However, we cannot
415 rule out the possibility that antibiotic stress contributed to plasmid loss. Among the diverse
416 mutations identified not affecting IMP MIC, some might have occurred by chance. However,
417 they might also have been selected as contributing to persistence or to an increased tolerance
418 like mutation in the lysine tRNA synthetase *lysS*.
419 In addition to mutants with similar MICs as the parental strains, we observed an extremely
420 broad range of mutations leading to increased MIC towards IMP, and, in most cases, also to
421 MEM. Resistant colonies could be classified according to their fitness based on their growth
422 rate, as determined by ScanLag (S1B Fig). Most isolates showing the less affected fitness under
423 the growth condition used (pattern A) were affected in OM permeability, with mutations in the
424 porin gene *ompK36*, but also in the Bam system and in the major chaperon involved in the
425 insertion of OMP in the OM. We also observed collateral effect of such mutations, like a
426 hypermucoid phenotype for the *bamA* mutant or increased mutation rate in the *polB* isolate.
427 Some mutations involving for instance regulatory systems and disrupting LPS biosynthesis
428 likely affected the OM permeability indirectly [51]. On the other hand, mutations from the B
429 pattern showed a strong fitness cost and are reminiscent of SCV. SCV have been described in
430 a broad range of species and are frequently associated with a decreased antibiotic susceptibility
431 [36]. However, there are only few reports of SCV in *K. pneumoniae*: in a bone and joint
432 infection [52] and associated with colistin HR in biofilm [53]. In both cases, the genetic bases
433 for the SCV phenotype were not identified. As reported in other species, most mutations we
434 have characterized affected aerobic respiration (quinone and heme biosynthesis) and the central
435 metabolism (TCA cycle and glycolysis). Interestingly, both the slow growth and the increased
436 MICs were fully or partially reversed in anaerobic conditions (S5 Table). The combination of

437 high resistance in the presence of oxygen and normal growth in its absence might contribute to
438 the selection of such mutation during treatment. However, due to their slow growth under
439 laboratory conditions, they might have been overlooked during diagnosis.
440 The increased MICs observed among HR colonies was shown to be frequently unstable and
441 lost following passages in antibiotic-free medium [14]. For different bacteria/antibiotic pairs,
442 HR was shown to result mainly from genomic amplification [34], which can revert by
443 homologous recombination between duplications. Here, we identified only four cases of
444 amplification. The duplication of the CTX-M-15 plasmid region carrying fitness functions
445 might have favored bacterial survival and be selected among colonies from the C-pattern
446 (persistent-like). Two amplifications were associated with a decreased susceptibility to IMP. In
447 the strain AC376, we observed a 89,584 bp duplication encompassing the *dcw* locus encoding
448 major functions for cell wall synthesis and cell division. Interestingly, the duplication was not
449 in tandem, but corresponded to an ectopic copy/paste of the region at position 688,936 (Fig. 5).
450 The insertion was located in the *ygiW* - *qseBC* intergenic region within *ygiW* ribosome binding
451 site (RBS). Interestingly, AC376 showed a 16-fold decrease of IMP susceptibility but almost
452 no effect on MEM susceptibility. This observation is in agreement with previous studies
453 showing that amplification of the *ftsQAZ* genes, part of the *dcw* locus, led to decreased
454 susceptibility to mecillinam, an antibiotic targeting exclusively PBP2 [54]. Indeed, both IMP
455 and MEM have a high affinity to PBP2, but MEM has also some further affinity to PBP3 [40].
456 In this case, the amplification and the phenotype were stable. Increased copy number of bla_{KPC}
457 was shown to lead to a higher MIC to carbapenems [10]. In strain AC150-A, we observed a 68
458 kb duplication within pKPC leading to a modest increase of IMP and MEM MICs (Fig. 5B, S4
459 Table). In addition, the 11 isolates with the highest pKPC coverage belong to pattern A but,
460 except for AC150-A, no change of IMP and MEM MICs was observed. The higher copy
461 number might have enhanced the survival on plates supplemented with IMP but it is predicted
462 to be unstable and likely not detectable in the experimental set-up we used.
463 For mutations leading to a high fitness cost, we observed frequent reversion of the growth defect
464 and the increased MICs. A typical case was strain AC90-A from the A pattern, which showed
465 MICs identical to the parental strain MICs and was mutated in both *cpxA* and in *cpxR*. The *cpxA*
466 mutation would have been first selected, leading to an hyperactivation of CpxR and in turn to
467 an overexpression of *acrB*, *acrD* and *eefB* efflux systems genes and a repression of the porin
468 gene *ompK36* [32]. However, the observed decreased susceptibility to carbapenems was
469 associated with a high fitness cost with the rapid accumulation of suppressor mutations. The
470 secondary mutation in *cpxR*, leading to an increased susceptibility compared to the parental

471 strain, suppresses the effect of the cpxA mutation and compensates for the high cost of the
472 primary mutation. This situation correspond to HR resulting of a mutations with a high fitness
473 cost suppressed by a secondary mutation also reverting the effect on antibiotic susceptibility
474 [14].
475
476 **Conclusion**: HR to IMP in KPC-Kp is the result of a combination of different mechanisms to
477 escape bactericidal antibiotics: collective protection effects, tolerance, persistence and
478 resistance. Inter-strain variations leading to different HR frequencies across the clinical isolates
479 here analyzed reflect the different bacterial response to IMP stress and is likely due to genetic
480 differences that remain to be characterized. The analysis of the bacterial response to antibiotics
481 on solid media compared to liquid culture allows to address the diversity of phenotypes and
482 genotypes of surviving bacteria. Although the majority of colonies did not show any genetic
483 change compared to the parental strains, we observed mutations in a very broad range of
484 functions considerably extending our knowledge of *K. pneumoniae* intrinsic ß-lactam
485 resistome. We hypothesize that mutations affecting these functions might also contribute to
486 IMP treatment failure in patients infected by KPC-Kp isolates.
487
488
489 **METHODS**
490
491 ***Klebsiella pneumoniae* isolates, media and growth conditions.** The isolates analyzed in this
492 work and their main characteristics are listed in S1 Table. It includes 62 KPC-Kp clinical
493 isolates and for comparison, 20 clinical isolates expressing other carbapenemases (OXA-48,
494 n=3; VIM-1, n=11; NDM-1, n=3; isolates co-carrying two carbapenemases, n=3) and three
495 isolates not carrying any carbapenemase gene as control. Bacteria were grown in Mueller-
496 Hinton (MH), Tryptic-Soy Broth (TSB) or Lysogeny broth (LB) and on Tryptic-Soy agar (TSA)
497 or LB agar (LBA) plates. Anaerobic growth was performed in an anaerobic chamber (Genbox
498 BioMérieux SA, Marcy/Etoile, France) by following the manufacturer instructions. Antibiotic
499 susceptibility testing (AST) was performed by Etest (BioMérieux) on Mueller-Hinton Agar
500 (MHA) plates inoculated by flood with 2 ml of bacterial culture (10^6 bacteria/ml). Flood
501 inoculation was selected instead of swab streaking to provide a more uniform inoculation.
502 Imipenem and meropenem breakpoints were according to the EUCAST guidelines
503 (https://www.eucast.org/) Susceptible, $\leq$2 mg/L and Resistant, $\geq$4 mg/l. Etest experiments also
504 allowed a preliminary screening for HR. We referred to HR as the occurrence of at least 5

505 colonies within the inhibition halo after 16-20 hours of incubation at 37 °C. Isolates with 3 or
506 4 colonies were defined as "moderately HR" and isolates with less than 3 colonies in the halo
507 were classified as "non HR". Isolates showing full contact with the Etest gradient strip for which
508 HR could not be detected were excluded from the analysis (S1 Table).
509 Plasmid pKPC stability in strain CNR146C9 was determined by quantifying growth of 194
510 independent colonies isolated on LB plates in LB medium supplemented with 0.5 mg/l MEM.
511 Strain AC420-C which have lost pKPC was used as non-growing control.
512
513 **Population Analysis Profiling (PAP).** Heteroresistance was quantified by PAP, following
514 spreading on agar plate of either stationary phase (SP) bacterial cultures (overnight culture, ON)
515 or exponentially growing bacteria (ON culture diluted 1000 times in TSB and incubated at 37°C
516 until OD_{600}~0.3-0.4 was reached). Bacterial cultures were serially diluted in saline buffer and
517 100 µl of dilution at OD_{600} of 0.01 (an estimate of 10^7 bacteria/ml) were spread evenly using
518 the automatic plater EasySpiral (Interscience) on freshly prepared TSA plates containing IMP
519 at 4-fold, 8-fold and 10-fold the MIC of each isolate, as determined by Etest. The plates were
520 incubated at 37 °C, and colonies were counted at 24 hours., The frequency of survival was
521 calculated as the ratio of CFUs on IMP supplemented medium over CFUs on media without
522 IMP. Given the uncertainty in determining CFUs, we arbitrary set a threshold of 10 colonies
523 per plate (10^2 CFU/ml) for significance. Results were calculated from five independent
524 experiments and expressed as the $\log_{10}$ of the frequency.
525
526 **ScanLag assay and data analysis.** ScanLag assays were performed as described previously
527 [24], but adapted to our purposes: approximately 1-3 x 10^6 cells from mid-EP or SP cultures
528 were spread onto TSA plates supplemented with IMP using the EasySpiral plater. Colony
529 tracking was carried out every 20 minutes for 48-hours at 37 °C. Time of appearance (ToA)
530 and colony growth rates were estimated by running MATLAB scripts publicly available at
531 https://github.com/iosonofabio/scanlag [55].
532 Colony ToA distributions were analyzed by using the R package *mixtools* [56]. We applied a
533 two-component mixture model to the ToA distributions of both untreated populations and those
534 surviving IMP exposure using expectation–maximization (EM) algorithm by the *normalmixEM*
535 function. Briefly, we jointly estimated the vectors of means μ (estimated ToA mean in each
536 component) and standard deviations Σ as well as the mixing weights λ (corresponding to the
537 initial proportion of colonies, expressed in %) to analyze and quantitatively compare
538 subpopulations across the selected isolates. The delay in growth of IMP exposed populations

539 compared to untreated colonies, hereto referred to as Lag time extension (LE), was quantified
540 as the ratio of mean ToA of N1 cells (first appearing population on IMP plates) over the mean
541 ToA of untreated colonies. The "persister" fraction was estimated using thresholds as
542 previously described [28]. Briefly, colonies were considered as deriving from persister cells if
543 they appeared later than three standard deviations away from the mean ToA of the N1
544 population (ToA > $\mu_{N1}+3\Sigma_{N1}$). Persister frequency over the whole population was calculated
545 per each isolate; data were then visualized using *ggplot2* [57].
546
547 **Isolation of surviving colonies.** Surviving colonies were selected from IMP-containing plates,
548 re-isolated on media containing the same IMP concentration and, in parallel, on drug free
549 media. The next day, colonies were picked from IMP plates or from plates without IMP - if the
550 colony did not grow on the IMP plate, and incubated in TSB without antibiotic until mid-
551 exponential phase was reached. The cultures were then used for AST by Etest and DNA
552 extraction for genome sequencing.
553
554 **Whole-genome sequencing and analysis.** Genomic DNAs were extracted by using the
555 DNeasy Blood & Tissue Kit (QIAGEN). *K. pneumoniae* genomes were sequenced by using the
556 Illumina HiSeq2500 or NextSeq500 platform, with 100- and 75-nucleotides (nt) paired-end
557 reads respectively. Libraries of *K. pneumoniae* clinical isolates were constructed by using the
558 Nextera XT kit (Illumina) and libraries of CNR146C9 clones selected during ScanLag
559 experiments by using NEBNext Ultra II FS DNA Library prep kit, which provide a more even
560 genome coverage [58]. Paired-end reads were assembled into contigs with SPAdes 3.9.0 [59].
561 The complete genome sequence of CNR146C9 was determined by using the long-read PacBio
562 technology. Accurate consensus reads obtained from raw reads with pbccs
563 (https://github.com/nlhepler/pbccs) were assembled with Canu [60]. The assembly was
564 polished with Circulator [61] and manually corrected by mapping Illumina reads with Breseq
565 0.33.2 [62]. Variants compared to CNR146C9 complete genome sequence were identified by
566 using Breseq [62]. Missing regions and recombination events were identified by analysing the
567 "Unassigned missing coverage evidence" and "Unassigned new junction evidence" sections of
568 the Breseq outputs respectively. Polymorphisms were visually verified by using Tablet [63].
569 Genome sequences were annotated with Prokka 1.14.5 [64] and analysed for MLST and ARG
570 content by using Kleborate [65] and Resfinder 4.0.1 [66]. Plasmid incompatibility groups were
571 identified by using PlasmidFinder 2.1 [67]. Copy number variation was estimated by counting

572 the number of reads per gene and comparing with number of Illumina reads of the parental
573 strain CNR146C9 by using the DESSeq2 R Package [68].
574
575 **Statistical analyses**. All statistical tests and graphical representations were performed using R
576 4.0.3 with R studio 1.3.1093 [69]. All statistical tests and graphical representations were
577 performed using R v.4.0-3 [69] using packages *ggplot2* [57] and *ggpubr*
578 (https://rpkgs.datanovia.com/ggpubr/index.html). The log10-transformed distributions of
579 survival frequency for exponentially-growing and stationary phases were compared using
580 Student's T-test. A *p-value* below the 5% threshold was deemed significant.
581
582 **Availability of data**. Sequence data for the clinical isolates have been deposited at
583 DDBJ/EMBL/GenBank (Bioproject ERP133503). CNR146C9 WGS was deposited with the
584 following accession numbers: ERS9645073. Biosamples for the Illumina sequence data are
585 listed in S1 Table.
586
587 **ACKNOWLEDGEMENTS**
588 This work was supported by grants from the French National Research Agency IBEID (ANR-
589 10-LABX-62-IBEID) and SEQ2DIAG (ANR-20-PAMR-0010). Adriana Chiarelli is part of the
590 Pasteur - Paris University (PPU) International PhD Program, with funding from the Institut
591 Carnot Pasteur Microbes & Santé, and the European Union's Horizon 2020 research and
592 innovation programme under the Marie Sklodowska-Curie grant agreement No 665807.
593 The authors thank Virgile Andreani and Gregory Bath for discussion on HR, Guilhem Royer
594 for critical reading of the manuscript, Laurence Ma from the Institut Pasteur Biomics platform
595 (C2RT, Institut Pasteur, Paris, France, supported by France Génomique, ANR-10-INBS-09-09
596 and IBISA) for her help with Illumina sequencing.
597
598 **BIBLIOGRAPHY**
599
600 1. Tacconelli E, Carrara E, Savoldi A, Harbarth S, Mendelson M, Monnet DL, et al. Discovery,
601 research, and development of new antibiotics: the WHO priority list of antibiotic-resistant bacteria and
602 tuberculosis. Lancet Infect Dis. 2018;18(3):318-27. Epub 2017/12/26. doi: 10.1016/s1473-
603 3099(17)30753-3. PubMed PMID: 29276051.
604 2. Nordmann P, Dortet L, Poirel L. Carbapenem resistance in Enterobacteriaceae: here is the
605 storm! Trends in molecular medicine. 2012;18(5):263-72. Epub 2012/04/07. doi:
606 10.1016/j.molmed.2012.03.003. PubMed PMID: 22480775.

3. Munoz-Price LS, Poirel L, Bonomo RA, Schwaber MJ, Daikos GL, Cormican M, et al. Clinical epidemiology of the global expansion of *Klebsiella pneumoniae* carbapenemases. Lancet Infect Dis. 2013;13(9):785-96. Epub 2013/08/24. doi: 10.1016/s1473-3099(13)70190-7. PubMed PMID: 23969216; PubMed Central PMCID: PMCPMC4673667.

4. Bush K, Jacoby GA. Updated functional classification of beta-lactamases. Antimicrob Agents Chemother. 2010;54(3):969-76. Epub 2009/12/10. doi: 10.1128/aac.01009-09. PubMed PMID: 19995920; PubMed Central PMCID: PMCPMC2825993.

5. David S, Reuter S, Harris SR, Glasner C, Feltwell T, Argimon S, et al. Epidemic of carbapenem-resistant *Klebsiella pneumoniae* in Europe is driven by nosocomial spread. Nature microbiology. 2019;4(11):1919-29. Epub 2019/07/31. doi: 10.1038/s41564-019-0492-8. PubMed PMID: 31358985.

6. Bonnin RA, Jousset AB, Chiarelli A, Emeraud C, Glaser P, Naas T, et al. Emergence of New Non-Clonal Group 258 High-Risk Clones among *Klebsiella pneumoniae* Carbapenemase-Producing *K. pneumoniae* Isolates, France. Emerg Infect Dis. 2020;26(6):1212-20. Epub 2020/05/23. doi: 10.3201/eid2606.191517. PubMed PMID: 32441629; PubMed Central PMCID: PMCPMC7258464.

7. Bassetti M, Peghin M. How to manage KPC infections. Therapeutic advances in infectious disease. 2020;7:2049936120912049. Epub 2020/06/04. doi: 10.1177/2049936120912049. PubMed PMID: 32489663; PubMed Central PMCID: PMCPMC7238785.

8. Kowalska-Krochmal B, Dudek-Wicher R. The Minimum Inhibitory Concentration of Antibiotics: Methods, Interpretation, Clinical Relevance. Pathogens (Basel, Switzerland). 2021;10(2). Epub 2021/02/10. doi: 10.3390/pathogens10020165. PubMed PMID: 33557078; PubMed Central PMCID: PMCPMC7913839.

9. Nordmann P, Cuzon G, Naas T. The real threat of *Klebsiella pneumoniae* carbapenemase-producing bacteria. Lancet Infect Dis. 2009;9(4):228-36. Epub 2009/03/28. doi: 10.1016/s1473-3099(09)70054-4. PubMed PMID: 19324295.

10. Bulman ZP, Krapp F, Pincus NB, Wenzler E, Murphy KR, Qi C, et al. Genomic Features Associated with the Degree of Phenotypic Resistance to Carbapenems in Carbapenem-Resistant *Klebsiella pneumoniae*. mSystems. 2021;6(5):e0019421. Epub 2021/09/15. doi: 10.1128/mSystems.00194-21. PubMed PMID: 34519526; PubMed Central PMCID: PMCPMC8547452.

11. Dewachter L, Fauvart M, Michiels J. Bacterial Heterogeneity and Antibiotic Survival: Understanding and Combatting Persistence and Heteroresistance. Molecular cell. 2019;76(2):255-67. Epub 2019/10/19. doi: 10.1016/j.molcel.2019.09.028. PubMed PMID: 31626749.

12. Bódi Z, Farkas Z, Nevozhay D, Kalapis D, Lázár V, Csörgő B, et al. Phenotypic heterogeneity promotes adaptive evolution. PLoS biology. 2017;15(5):e2000644. Epub 2017/05/10. doi: 10.1371/journal.pbio.2000644. PubMed PMID: 28486496; PubMed Central PMCID: PMCPMC5423553.

13. Band VI, Weiss DS. Heteroresistance: A cause of unexplained antibiotic treatment failure? PLoS Pathog. 2019;15(6):e1007726. Epub 2019/06/07. doi: 10.1371/journal.ppat.1007726. PubMed PMID: 31170271; PubMed Central PMCID: PMCPMC6553791 applications related to heteroresistance.

14. Andersson DI, Nicoloff H, Hjort K. Mechanisms and clinical relevance of bacterial heteroresistance. Nat Rev Microbiol. 2019;17(8):479-96. Epub 2019/06/27. doi: 10.1038/s41579-019-0218-1. PubMed PMID: 31235888.

15. Band VI, Satola SW, Smith RD, Hufnagel DA, Bower C, Conley AB, et al. Colistin Heteroresistance Is Largely Undetected among Carbapenem-Resistant *Enterobacterales* in the United States. mBio. 2021;12(1). Epub 2021/01/28. doi: 10.1128/mBio.02881-20. PubMed PMID: 33500343; PubMed Central PMCID: PMCPMC7858057.

16. Bardet L, Baron S, Leangapichart T, Okdah L, Diene SM, Rolain JM. Deciphering Heteroresistance to Colistin in a *Klebsiella pneumoniae* Isolate from Marseille, France. Antimicrob Agents Chemother. 2017;61(6). Epub 2017/04/19. doi: 10.1128/aac.00356-17. PubMed PMID: 28416544; PubMed Central PMCID: PMCPMC5444162.

658 17. Tan K, Nguyen J, Nguyen K, Huse HK, Nieberg PH, Wong-Beringer A. Prevalence of the
659 carbapenem-heteroresistant phenotype among ESBL-producing *Escherichia coli* and *Klebsiella*
660 *pneumoniae* clinical isolates. J Antimicrob Chemother. 2020;75(6):1506-12. Epub 2020/03/18. doi:
661 10.1093/jac/dkaa048. PubMed PMID: 32181802.

662 18. López-Camacho E, Paño-Pardo JR, Sotillo A, Elías-López C, Martínez-Martínez L, Gómez-Gil
663 R, et al. Meropenem heteroresistance in clinical isolates of OXA-48-producing *Klebsiella pneumoniae*.
664 Diagnostic microbiology and infectious disease. 2019;93(2):162-6. Epub 2018/10/10. doi:
665 10.1016/j.diagmicrobio.2018.09.008. PubMed PMID: 30297092.

666 19. Nodari CS, Ribeiro VB, Barth AL. Imipenem heteroresistance: high prevalence among
667 Enterobacteriaceae *Klebsiella pneumoniae* carbapenemase producers. J Med Microbiol. 2015;64(Pt
668 1):124-6. Epub 2014/10/30. doi: 10.1099/jmm.0.081869-0. PubMed PMID: 25351714.

669 20. Pournaras S, Kristo I, Vrioni G, Ikonomidis A, Poulou A, Petropoulou D, et al. Characteristics
670 of meropenem heteroresistance in *Klebsiella pneumoniae* carbapenemase (KPC)-producing clinical
671 isolates of *K. pneumoniae*. J Clin Microbiol. 2010;48(7):2601-4. Epub 2010/05/28. doi:
672 10.1128/jcm.02134-09. PubMed PMID: 20504985; PubMed Central PMCID: PMCPMC2897536.

673 21. Adams-Sapper S, Nolen S, Donzelli GF, Lal M, Chen K, Justo da Silva LH, et al. Rapid
674 induction of high-level carbapenem resistance in heteroresistant KPC-producing *Klebsiella*
675 *pneumoniae*. Antimicrob Agents Chemother. 2015;59(6):3281-9. Epub 2015/03/25. doi:
676 10.1128/aac.05100-14. PubMed PMID: 25801565; PubMed Central PMCID: PMCPMC4432212.

677 22. Adams-Sapper S, Gayoso A, Riley LW. Stress-Adaptive Responses Associated with High-
678 Level Carbapenem Resistance in KPC-Producing *Klebsiella pneumoniae*. Journal of pathogens.
679 2018;2018:3028290. Epub 2018/04/17. doi: 10.1155/2018/3028290. PubMed PMID: 29657865;
680 PubMed Central PMCID: PMCPMC5883989.

681 23. Nicoloff H, Andersson DI. Indirect resistance to several classes of antibiotics in cocultures with
682 resistant bacteria expressing antibiotic-modifying or -degrading enzymes. J Antimicrob Chemother.
683 2016;71(1):100-10. Epub 2015/10/16. doi: 10.1093/jac/dkv312. PubMed PMID: 26467993.

684 24. Levin-Reisman I, Gefen O, Fridman O, Ronin I, Shwa D, Sheftel H, et al. Automated imaging
685 with ScanLag reveals previously undetectable bacterial growth phenotypes. Nature methods.
686 2010;7(9):737-9. Epub 2010/08/03. doi: 10.1038/nmeth.1485. PubMed PMID: 20676109.

687 25. Fajardo-Lubian A, Ben Zakour NL, Agyekum A, Qi Q, Iredell JR. Host adaptation and
688 convergent evolution increases antibiotic resistance without loss of virulence in a major human
689 pathogen. PLoS Pathog. 2019;15(3):e1007218. Epub 2019/03/16. doi: 10.1371/journal.ppat.1007218.
690 PubMed PMID: 30875398; PubMed Central PMCID: PMCPMC6436753.

691 26. Steward CD, Mohammed JM, Swenson JM, Stocker SA, Williams PP, Gaynes RP, et al.
692 Antimicrobial susceptibility testing of carbapenems: multicenter validity testing and accuracy levels of
693 five antimicrobial test methods for detecting resistance in Enterobacteriaceae and Pseudomonas
694 aeruginosa isolates. J Clin Microbiol. 2003;41(1):351-8. Epub 2003/01/09. doi: 10.1128/jcm.41.1.351-
695 358.2003. PubMed PMID: 12517872; PubMed Central PMCID: PMCPMC149638.

696 27. Anderl JN, Zahller J, Roe F, Stewart PS. Role of nutrient limitation and stationary-phase
697 existence in *Klebsiella pneumoniae* biofilm resistance to ampicillin and ciprofloxacin. Antimicrob
698 Agents Chemother. 2003;47(4):1251-6. Epub 2003/03/26. doi: 10.1128/aac.47.4.1251-1256.2003.
699 PubMed PMID: 12654654; PubMed Central PMCID: PMCPMC152508.

700 28. Levin-Reisman I, Balaban NQ. Quantitative Measurements of Type I and Type II Persisters
701 Using ScanLag. Methods Mol Biol. 2016;1333:75-81. Epub 2015/10/16. doi: 10.1007/978-1-4939-
702 2854-5_7. PubMed PMID: 26468101.

703 29. Villa L, Feudi C, Fortini D, Brisse S, Passet V, Bonura C, et al. Diversity, virulence, and
704 antimicrobial resistance of the KPC-producing *Klebsiella pneumoniae* ST307 clone. Microbial
705 genomics. 2017;3(4):e000110. Epub 2017/08/09. doi: 10.1099/mgen.0.000110. PubMed PMID:
706 28785421; PubMed Central PMCID: PMCPMC5506382.

707 30. Hagan CL, Silhavy TJ, Kahne D. β-Barrel membrane protein assembly by the Bam complex.
708 Annu Rev Biochem. 2011;80:189-210. Epub 2011/03/05. doi: 10.1146/annurev-biochem-061408-
709 144611. PubMed PMID: 21370981.

31. Denoncin K, Schwalm J, Vertommen D, Silhavy TJ, Collet JF. Dissecting the Escherichia coli periplasmic chaperone network using differential proteomics. Proteomics. 2012;12(9):1391-401. Epub 2012/05/17. doi: 10.1002/pmic.201100633. PubMed PMID: 22589188; PubMed Central PMCID: PMCPMC3883104.

32. Srinivasan VB, Vaidyanathan V, Mondal A, Rajamohan G. Role of the two component signal transduction system CpxAR in conferring cefepime and chloramphenicol resistance in *Klebsiella pneumoniae* NTUH-K2044. PLoS One. 2012;7(4):e33777. Epub 2012/04/13. doi: 10.1371/journal.pone.0033777. PubMed PMID: 22496764; PubMed Central PMCID: PMCPMC3319533.

33. Vogt SL, Raivio TL. Just scratching the surface: an expanding view of the Cpx envelope stress response. FEMS Microbiol Lett. 2012;326(1):2-11. Epub 2011/11/19. doi: 10.1111/j.1574-6968.2011.02406.x. PubMed PMID: 22092948.

34. Nicoloff H, Hjort K, Levin BR, Andersson DI. The high prevalence of antibiotic heteroresistance in pathogenic bacteria is mainly caused by gene amplification. Nature microbiology. 2019;4(3):504-14. Epub 2019/02/12. doi: 10.1038/s41564-018-0342-0. PubMed PMID: 30742072.

35. Gershanovitch VN, Yourovitskaya NV, Komissarova LV, Bolshakova TN, Erlagaeva RS, Bourd GI. Catabolite repression in *Escherichia coli* K12 mutants defective in glucose transport. Mol Gen Genet. 1975;140(1):81-90. Epub 1975/09/15. doi: 10.1007/bf00268991. PubMed PMID: 1102954.

36. Proctor RA, von Eiff C, Kahl BC, Becker K, McNamara P, Herrmann M, et al. Small colony variants: a pathogenic form of bacteria that facilitates persistent and recurrent infections. Nat Rev Microbiol. 2006;4(4):295-305. Epub 2006/03/17. doi: 10.1038/nrmicro1384. PubMed PMID: 16541137.

37. Kneidinger B, Marolda C, Graninger M, Zamyatina A, McArthur F, Kosma P, et al. Biosynthesis pathway of ADP-L-glycero-beta-D-manno-heptose in *Escherichia coli*. J Bacteriol. 2002;184(2):363-9. Epub 2001/12/26. doi: 10.1128/jb.184.2.363-369.2002. PubMed PMID: 11751812; PubMed Central PMCID: PMCPMC139585.

38. Thulin E, Sundqvist M, Andersson DI. Amdinocillin (Mecillinam) resistance mutations in clinical isolates and laboratory-selected mutants of *Escherichia coli*. Antimicrob Agents Chemother. 2015;59(3):1718-27. Epub 2015/01/15. doi: 10.1128/aac.04819-14. PubMed PMID: 25583718; PubMed Central PMCID: PMCPMC4325821.

39. Sutaria DS, Moya B, Green KB, Kim TH, Tao X, Jiao Y, et al. First Penicillin-Binding Protein Occupancy Patterns of β-Lactams and β-Lactamase Inhibitors in *Klebsiella pneumoniae*. Antimicrob Agents Chemother. 2018;62(6). Epub 2018/05/02. doi: 10.1128/aac.00282-18. PubMed PMID: 29712652; PubMed Central PMCID: PMCPMC5971569.

40. Sumita Y, Fukasawa M, Okuda T. Comparison of two carbapenems, SM-7338 and imipenem: affinities for penicillin-binding proteins and morphological changes. The Journal of antibiotics. 1990;43(3):314-20. Epub 1990/03/01. doi: 10.7164/antibiotics.43.314. PubMed PMID: 2108953.

41. Zhanel GG, Wiebe R, Dilay L, Thomson K, Rubinstein E, Hoban DJ, et al. Comparative review of the carbapenems. Drugs. 2007;67(7):1027-52. Epub 2007/05/10. doi: 10.2165/00003495-200767070-00006. PubMed PMID: 17488146.

42. Nickolai DJ, Lammel CJ, Byford BA, Morris JH, Kaplan EB, Hadley WK, et al. Effects of storage temperature and pH on the stability of eleven beta-lactam antibiotics in MIC trays. J Clin Microbiol. 1985;21(3):366-70. Epub 1985/03/01. doi: 10.1128/jcm.21.3.366-370.1985. PubMed PMID: 3980689; PubMed Central PMCID: PMCPMC271666.

43. Mehta SC, Rice K, Palzkill T. Natural Variants of the KPC-2 Carbapenemase have Evolved Increased Catalytic Efficiency for Ceftazidime Hydrolysis at the Cost of Enzyme Stability. PLoS Pathog. 2015;11(6):e1004949. Epub 2015/06/02. doi: 10.1371/journal.ppat.1004949. PubMed PMID: 26030609; PubMed Central PMCID: PMCPMC4452179.

44. Wang P, Robert L, Pelletier J, Dang WL, Taddei F, Wright A, et al. Robust growth of Escherichia coli. Current biology : CB. 2010;20(12):1099-103. Epub 2010/06/12. doi: 10.1016/j.cub.2010.04.045. PubMed PMID: 20537537; PubMed Central PMCID: PMCPMC2902570.

761 45. Fridman O, Goldberg A, Ronin I, Shoresh N, Balaban NQ. Optimization of lag time underlies
762 antibiotic tolerance in evolved bacterial populations. Nature. 2014;513(7518):418-21. Epub 2014/07/22.
763 doi: 10.1038/nature13469. PubMed PMID: 25043002.

764 46. Levin-Reisman I, Brauner A, Ronin I, Balaban NQ. Epistasis between antibiotic tolerance,
765 persistence, and resistance mutations. Proc Natl Acad Sci U S A. 2019;116(29):14734-9. Epub
766 2019/07/03. doi: 10.1073/pnas.1906169116. PubMed PMID: 31262806; PubMed Central PMCID:
767 PMCPMC6642377.

768 47. Levin-Reisman I, Ronin I, Gefen O, Braniss I, Shoresh N, Balaban NQ. Antibiotic tolerance
769 facilitates the evolution of resistance. Science. 2017;355(6327):826-30. Epub 2017/02/12. doi:
770 10.1126/science.aaj2191. PubMed PMID: 28183996.

771 48. Winther KS, Gerdes K. Enteric virulence associated protein VapC inhibits translation by
772 cleavage of initiator tRNA. Proc Natl Acad Sci U S A. 2011;108(18):7403-7. Epub 2011/04/20. doi:
773 10.1073/pnas.1019587108. PubMed PMID: 21502523; PubMed Central PMCID: PMCPMC3088637.

774 49. Gerdes K, Maisonneuve E. Bacterial persistence and toxin-antitoxin loci. Annu Rev Microbiol.
775 2012;66:103-23. Epub 2012/09/22. doi: 10.1146/annurev-micro-092611-150159. PubMed PMID:
776 22994490.

777 50. Jousset AB, Bonnin RA, Takissian J, Girlich D, Mihaila L, Cabanel N, et al. Concomitant
778 carriage of KPC-producing and non-KPC-producing *Klebsiella pneumoniae* ST512 within a single
779 patient. J Antimicrob Chemother. 2020;75(8):2087-92. Epub 2020/05/10. doi: 10.1093/jac/dkaa137.
780 PubMed PMID: 32386410.

781 51. Davin-Regli A, Guerin-Faublée V, Pagès JM. Modification of outer membrane permeability
782 and alteration of LPS in veterinary enterotoxigenic *Escherichia coli*. Research in veterinary science.
783 2019;124:321-7. Epub 2019/04/30. doi: 10.1016/j.rvsc.2019.04.011. PubMed PMID: 31035220.

784 52. Ronde-Oustau C, Lustig S, Dupieux C, Ferry T. Implant-associated ESBL-*Klebsiella*
785 *pneumonia* producing small colony variant bone and joint infection in a healthy 40-year-old man. BMJ
786 case reports. 2017;2017. Epub 2017/02/09. doi: 10.1136/bcr-2016-217542. PubMed PMID: 28167688;
787 PubMed Central PMCID: PMCPMC5293972.

788 53. Silva A, Sousa AM, Alves D, Lourenço A, Pereira MO. Heteroresistance to colistin in *Klebsiella*
789 *pneumoniae* is triggered by small colony variants sub-populations within biofilms. Pathogens and
790 disease. 2016;74(5). Epub 2016/05/04. doi: 10.1093/femspd/ftw036. PubMed PMID: 27140200.

791 54. Vinella D, Cashel M, D'Ari R. Selected amplification of the cell division genes *ftsQ-ftsA-ftsZ* in
792 *Escherichia coli*. Genetics. 2000;156(4):1483-92. Epub 2000/12/05. PubMed PMID: 11102351;
793 PubMed Central PMCID: PMCPMC1461353.

794 55. Levin-Reisman I, Fridman O, Balaban NQ. ScanLag: high-throughput quantification of colony
795 growth and lag time. Journal of visualized experiments : JoVE. 2014;(89). Epub 2014/08/01. doi:
796 10.3791/51456. PubMed PMID: 25077667; PubMed Central PMCID: PMCPMC4215631.

797 56. Benaglia T, Chauveau D, Hunter DR, Young DS. mixtools: An R Package for Analyzing
798 Mixture Models. Journal of Statistical Software. 2010;32(6). doi: 10.18637/jss.v032.i06.

799 57. Wickham HS, Berlin, 2009). ggplot2: Elegant Graphics for Data Analysis: Springer, Berlin;
800 2009.

801 58. Chiarelli A, Cabanel N, Rosinski-Chupin I, Zongo PD, Naas T, Bonnin RA, et al. Diversity of
802 mucoid to non-mucoid switch among carbapenemase-producing *Klebsiella pneumoniae*. BMC
803 Microbiol. 2020;20(1):325. Epub 2020/10/29. doi: 10.1186/s12866-020-02007-y. PubMed PMID:
804 33109078; PubMed Central PMCID: PMCPMC7590720.

805 59. Bankevich A, Nurk S, Antipov D, Gurevich AA, Dvorkin M, Kulikov AS, et al. SPAdes: a new
806 genome assembly algorithm and its applications to single-cell sequencing. Journal of computational
807 biology : a journal of computational molecular cell biology. 2012;19(5):455-77. Epub 2012/04/18. doi:
808 10.1089/cmb.2012.0021. PubMed PMID: 22506599; PubMed Central PMCID: PMCPMC3342519.

809 60. Koren S, Walenz BP, Berlin K, Miller JR, Bergman NH, Phillippy AM. Canu: scalable and
810 accurate long-read assembly via adaptive k-mer weighting and repeat separation. Genome Res.

811 2017;27(5):722-36. Epub 2017/03/17. doi: 10.1101/gr.215087.116. PubMed PMID: 28298431;
812 PubMed Central PMCID: PMCPMC5411767.
813 61. Hunt M, Silva ND, Otto TD, Parkhill J, Keane JA, Harris SR. Circlator: automated
814 circularization of genome assemblies using long sequencing reads. Genome Biol. 2015;16:294. Epub
815 2015/12/31. doi: 10.1186/s13059-015-0849-0. PubMed PMID: 26714481; PubMed Central PMCID:
816 PMCPMC4699355.
817 62. Deatherage DE, Barrick JE. Identification of mutations in laboratory-evolved microbes from
818 next-generation sequencing data using breseq. Methods Mol Biol. 2014;1151:165-88. Epub 2014/05/20.
819 doi: 10.1007/978-1-4939-0554-6_12. PubMed PMID: 24838886; PubMed Central PMCID:
820 PMCPMC4239701.
821 63. Milne I, Stephen G, Bayer M, Cock PJ, Pritchard L, Cardle L, et al. Using Tablet for visual
822 exploration of second-generation sequencing data. Briefings in bioinformatics. 2013;14(2):193-202.
823 Epub 2012/03/27. doi: 10.1093/bib/bbs012. PubMed PMID: 22445902.
824 64. Seemann T. Prokka: rapid prokaryotic genome annotation. Bioinformatics. 2014;30(14):2068-
825 9. Epub 2014/03/20. doi: 10.1093/bioinformatics/btu153. PubMed PMID: 24642063.
826 65. Wyres KL, Nguyen TNT, Lam MMC, Judd LM, van Vinh Chau N, Dance DAB, et al. Genomic
827 surveillance for hypervirulence and multi-drug resistance in invasive *Klebsiella pneumonia*e from South
828 and Southeast Asia. Genome Med. 2020;12(1):11. Epub 2020/01/18. doi: 10.1186/s13073-019-0706-y.
829 PubMed PMID: 31948471; PubMed Central PMCID: PMCPMC6966826.
830 66. Bortolaia V, Kaas RS, Ruppe E, Roberts MC, Schwarz S, Cattoir V, et al. ResFinder 4.0 for
831 predictions of phenotypes from genotypes. J Antimicrob Chemother. 2020. Epub 2020/08/12. doi:
832 10.1093/jac/dkaa345. PubMed PMID: 32780112.
833 67. Carattoli A, Zankari E, Garcia-Fernandez A, Voldby Larsen M, Lund O, Villa L, et al. In silico
834 detection and typing of plasmids using PlasmidFinder and plasmid multilocus sequence typing.
835 Antimicrob Agents Chemother. 2014;58(7):3895-903. Epub 2014/04/30. doi: 10.1128/aac.02412-14.
836 PubMed PMID: 24777092; PubMed Central PMCID: PMCPMC4068535.
837 68. Varet H, Brillet-Guéguen L, Coppée JY, Dillies MA. SARTools: A DESeq2- and EdgeR-Based
838 R Pipeline for Comprehensive Differential Analysis of RNA-Seq Data. PLoS One.
839 2016;11(6):e0157022. Epub 2016/06/10. doi: 10.1371/journal.pone.0157022. PubMed PMID:
840 27280887; PubMed Central PMCID: PMCPMC4900645.
841 69. Racine JS. RStudio: A Platform-Independent IDE for R and Sweave. Journal of Applied
842 Econometrics. 2012;27:167-72. doi: doi.org/10.1002/jae.1278.
843

844 **FIGURE LEGENDS**

845

846 **Fig 1. Diversity of resistance and heteroresistance.** (A) Visualization of the HR profiles by
847 Etest. Three different categories were distinguished (HR, moderate HR and absent HR). Isolates
848 showing full contact with the antibiotic strip (on the right) were excluded from further analyses
849 and classified as "HR not detectable" (S1 Table); (**B)** Occurrence of HR among KPC isolates.
850 SIR = Susceptible/Intermediate/Resistant. Bar colors: dark grey = imipenem (IMP), light grey
851 = meropenem (MEM). Yes = presence of HR (including HR and moderate HR isolates), No =
852 absence of HR. Isolates that showed full contact with the antibiotic strip (*n* = 31 for MEM and
853 *n* = 3 for IMP) were not included; (**C)** Correlation between HR profile and type of KPC
854 carbapenemase. Bar colors: Blue = KPC-2; Orange = KPC-3; yes for HR and no for non-HR.

855

856 **Fig. 2. Population analysis profiling (PAP) of 13 CPKp clinical isolates (A)** Results were
857 expressed in log_{10} of the frequency of survival at 4-FOLD, 8-FOLD, 10-FOLD the
858 concentration of IMP relative to the MIC of the isolate as determined by Etest. Isolates names
859 are indicated at the top of each chart. Red bars: KPC isolates; magenta bars: VIM isolates; green
860 bars: NDM isolates; blue bars: OXA isolates. The red dashed line indicates the cutoff value (-
861 5) above which counts were considered significant. (**B)** Impact of the bacterial growth phase on
862 the survival to different doses of imipenem. Green bars indicate plating from exponentially
863 growing cultures, whereas orange indicates plating from stationary phase bacterial cultures.
864 Data were calculated from five independent experiments. Significant results were highlighted:
865 * *p*-value ranging from 0.0159 to 0.0278; ** *p*-value ranging from 0.0025 to 0.093.

866

867 **Fig 3. Heterogeneous survival of KPC-Kp to high concentrations of IMP (A)** Histograms
868 of single-colony time of appearance from exponentially growing cultures. Colony appearance
869 time was monitored every 20 minute over 48-hours incubation on plate. ToA = Time of
870 Appearance; cyan blue bars represent colonies appearing on drug-free media, whereas red bars
871 indicate colonies growing onto IMP-containing agar plates. The data are an overlap of at least
872 three independent replicates per each isolate and each condition. (**B)** Fit of two-mixture
873 component model to the distributions of ToA for each isolates after plating from exponential
874 phase cultures. In red, population 1 (N1), and in blue the population 2 (N2). The representation
875 is an overlap of at least three independent replicates per isolate and per condition. ToA data are
876 expressed as density rather than count. Estimated parameters of each subpopulations and
877 replicates are given in S2 Table. Note that, for the isolate BIC-1, the model failed to fit a normal
878 distribution to the tail. (**C)** Comparison of Lag Time Extension (LE) of N1 subpopulations from
879 the six isolates plated from EP and SP cultures. Only significant differences were highlighted
880 (* corresponds to *p*-value = 0.033, ** corresponds to *p*-value = 0.0025). LE was calculated as
881 the mean ToA value of N1 population over the mean ToA value of untreated population. **(D)**
882 Frequency of persisters calculated according to the methodology proposed by Balaban et al
883 [28] from at least three replicates (data are available in Table S2). Colonies appearing after the
884 cutoff value (calculated as ToA > $\mu+3\Sigma$, where μ= estimated ToA mean for N1 and Σ =
885 estimated standard deviations) were defined as persisters. Frequencies were calculated as the
886 proportion of CFU/ml of each subpopulation over the total number of CFU/ml of the initial
887 inoculum. The frequency of persisters was significantly higher in exponential phase rather than
888 in stationary phase for CNR146C9 isolate (**, *p*-value = 0.0038).

889

890 **Fig 4. Diversity of genetic events detected among colonies from patterns A, B and C. (A)**
891 Diversity of genetic events as identified by using Breseq. **(B)** Functional categories of loci
892 affected by the genetic events as identified in S3, S4 and S5 Tables. The three classes of colonies
893 as defined by their ToA and growth rate, A, B and C are indicated in green, red and blue
894 respectively.

895

896 **Fig 5. DNA amplification and pKPC copy numbers in pattern A isolates.** (**A)** Duplication
897 of a 89584 bp region in strain AC376-A. The relative copy number was estimated compared to
898 the parental stain CNR146C9 based on the count of number of reads counted per gene. The
899 duplicated region is in blue and contains as candidate locus contributing to increased IMP MIC
900 the division and cell wall (dcw) locus (in orange). The insertion of the duplicated copy occurred
901 11 bp upstream *ygiW* with a 5 bp (GAGAA) duplication. *ygiW* expression is activated by the
902 two component regulatory system QseBC encoded by two genes in the opposite orientation.
903 Limits of the duplicated region and insertion sites were deduced from chimeric reads as
904 identified by using Breseq [62]**. (B)** Duplication of a c.a. 68 kb region within the pKPC plasmid
905 in strain AC150-A. Average copy number of the 115 CDS of pKPC was calculated relative to
906 the corresponding average value for all isolates except those having lost pKPC. The central part
907 of the duplicated region is highly similar to a pCTX-M-15 DNA regions lost in this strain and
908 explaining the variable and lower copy number as quantified by counting mapping reads (C)
909 Average copy number of pKPC CDSs compared to the average copy number of pKPC CDS
910 across all isolates, except those having lost pKPC. In blue, A isolates; in orange, B isolates and
911 in green, C isolates.

912

A

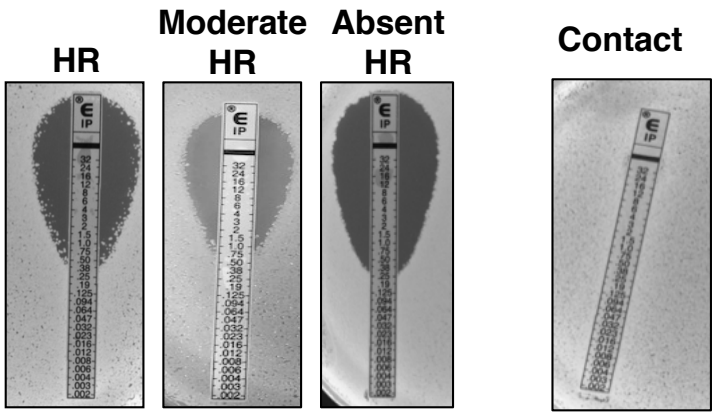
HR
Moderate HR
Absent HR
Contact

B

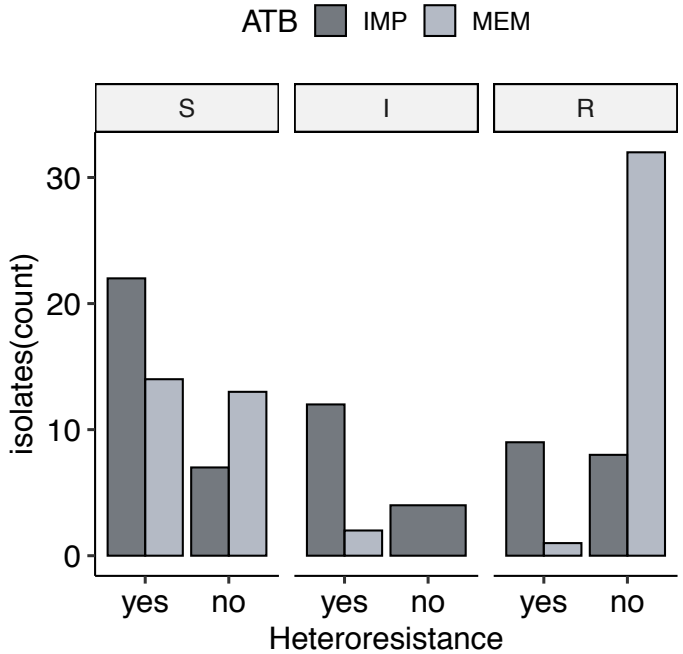
ATB
IMP
MEM
S
I
R
isolates(count)
0
10
20
30
yes
no
yes
no
yes
no
Heteroresistance

C

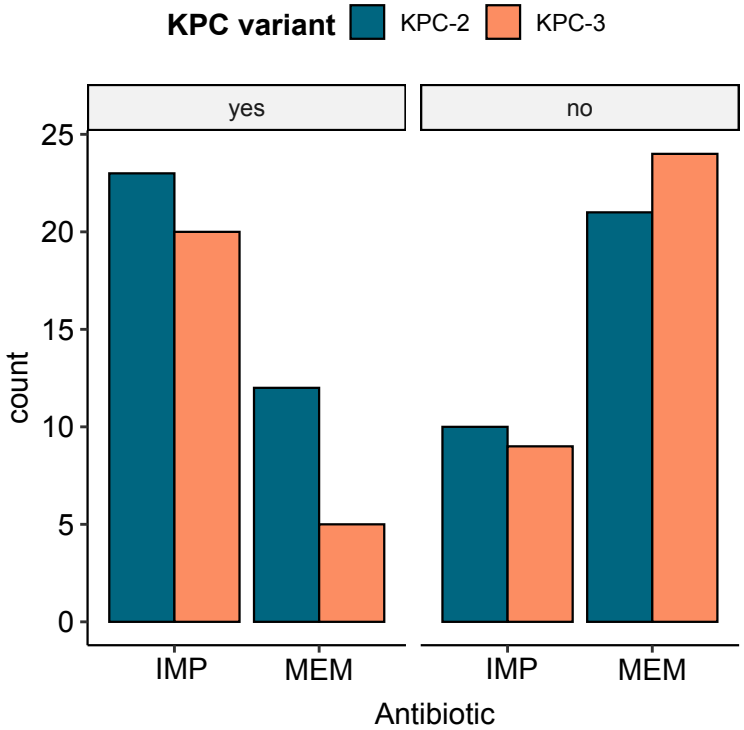
KPC variant
KPC-2
KPC-3
yes
no
count
0
5
10
15
20
25
IMP
MEM
IMP
MEM
Antibiotic

Fig.1

A

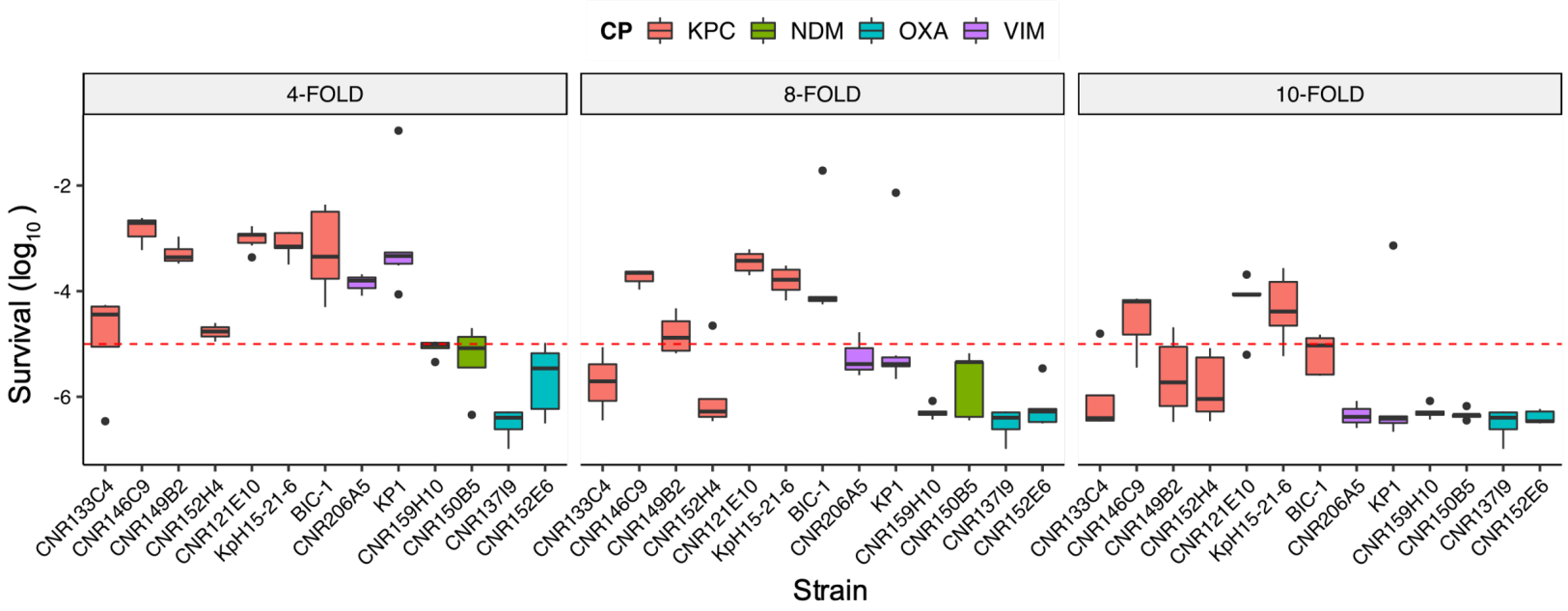
CP KPC NDM OXA VIM
4-FOLD
8-FOLD
10-FOLD
Survival (log10)
-2
-4
-6
CNR133C4
CNR146C9
CNR149B2
CNR152H4
CNR121E10
KpH15-21-6
BIC-1
CNR206A5
KP1
CNR159H10
CNR150B5
CNR137I9
CNR152E6
Strain

B

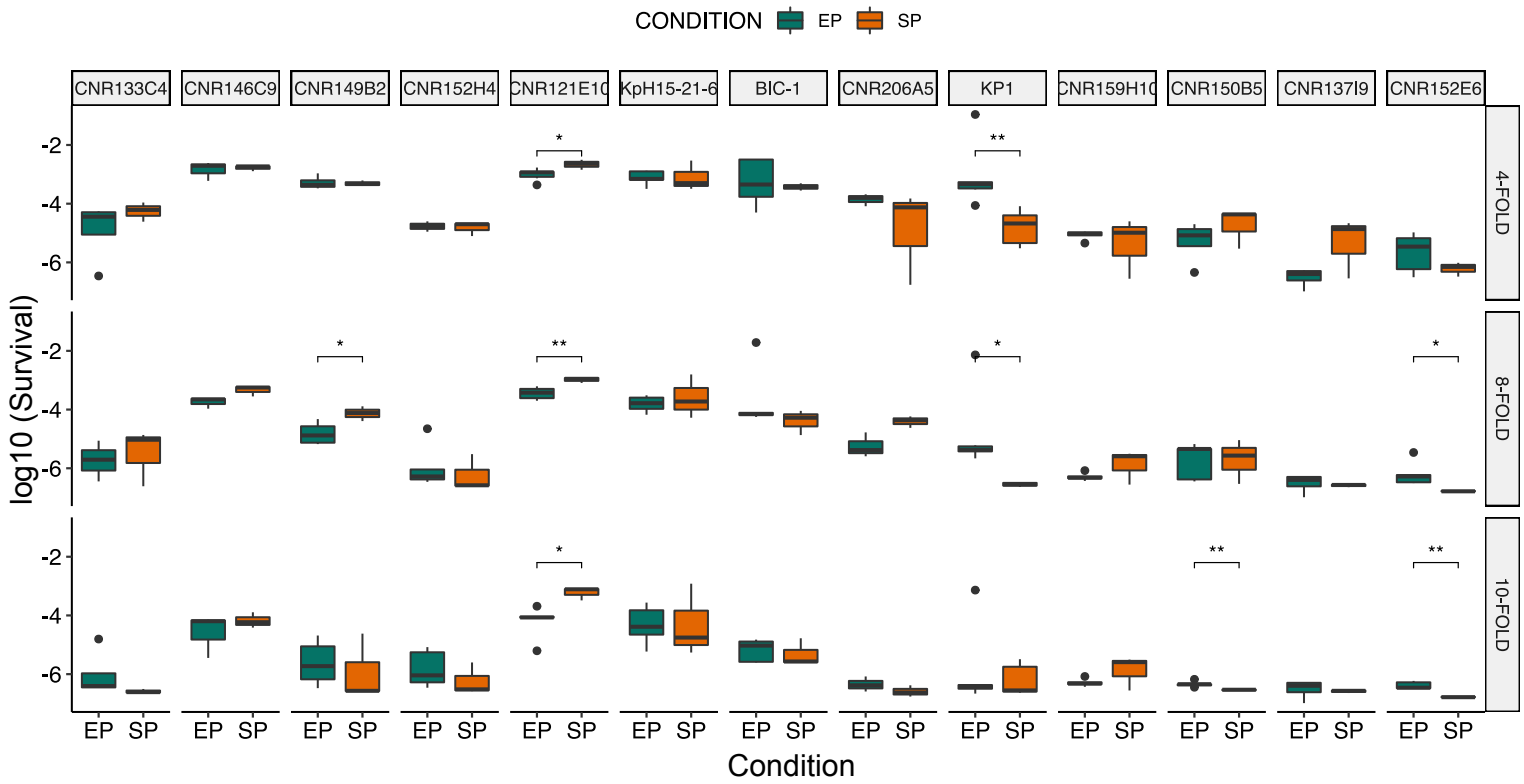
CONDITION EP SP
CNR133C4
CNR146C9
CNR149B2
CNR152H4
CNR121E10
KpH15-21-6
BIC-1
CNR206A5
KP1
CNR159H10
CNR150B5
CNR137I9
CNR152E6
4-FOLD
8-FOLD
10-FOLD
log10 (Survival)
-2
-4
-6
EP SP
Condition

Fig.2

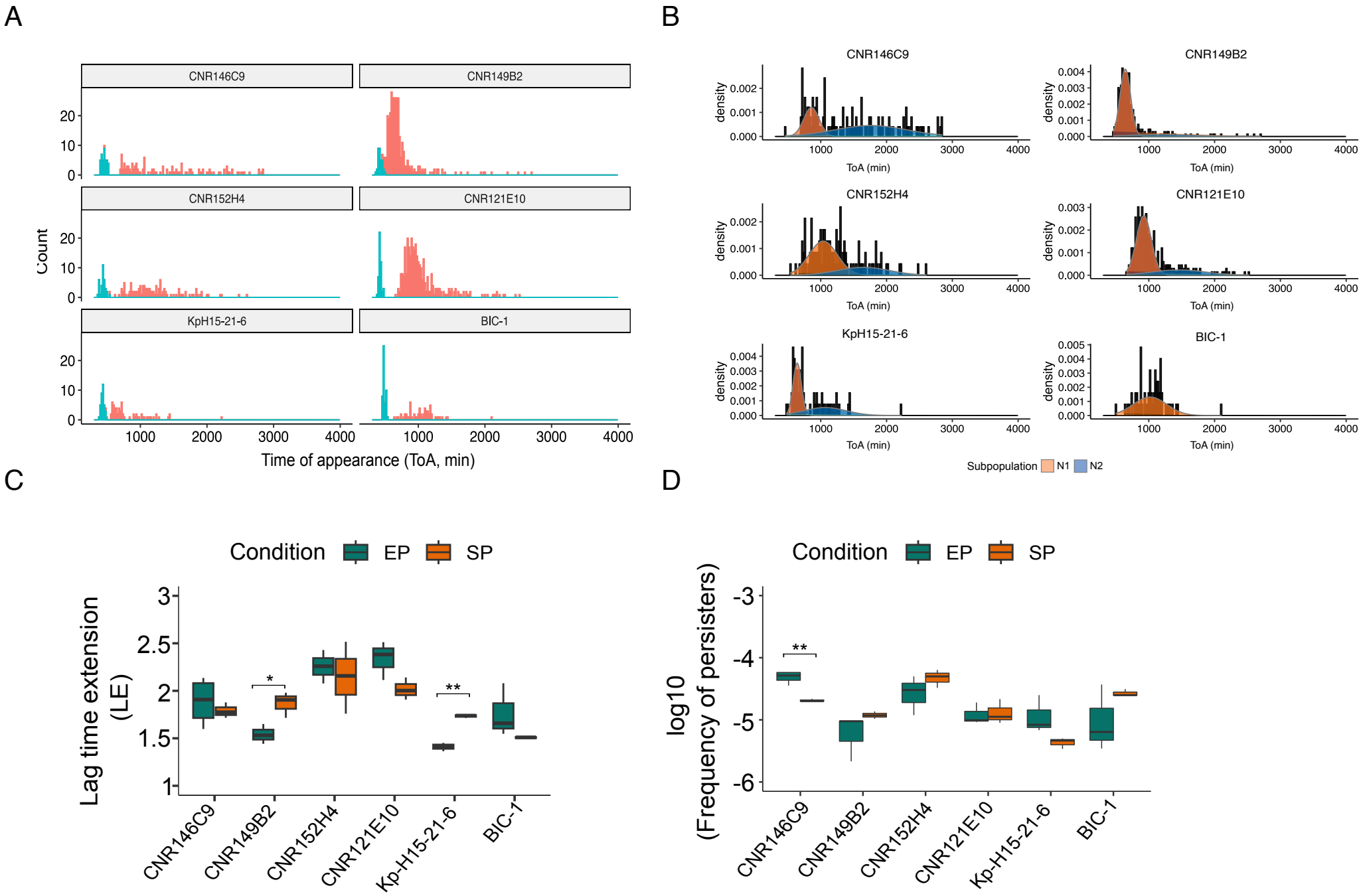
A
CNR146C9
CNR149B2
CNR152H4
CNR121E10
KpH15-21-6
BIC-1
Count
Time of appearance (ToA, min)
B
density
ToA (min)
Subpopulation N1 N2
C
Condition EP SP
Lag time extension (LE)
D
log10 (Frequency of persisters)

Fig.3

A

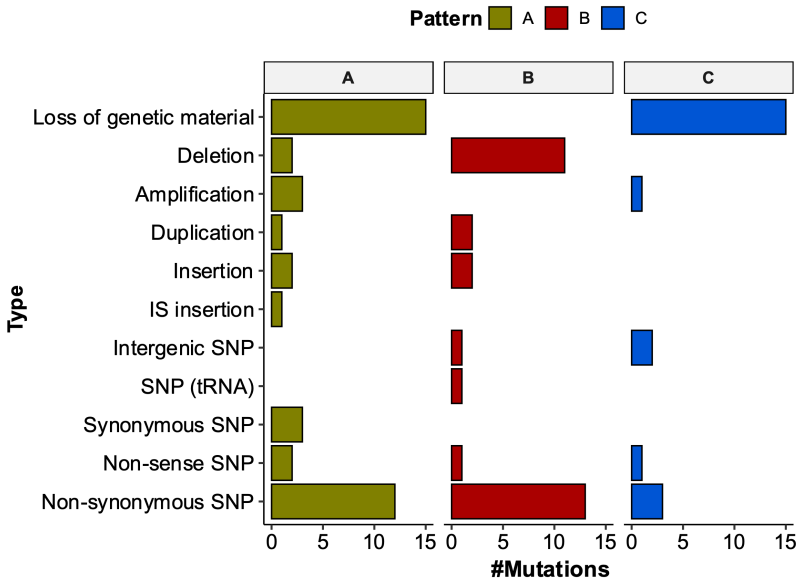
Pattern A B C
A
B
C
Loss of genetic material
Deletion
Amplification
Duplication
Insertion
IS insertion
Intergenic SNP
SNP (tRNA)
Synonymous SNP
Non-sense SNP
Non-synonymous SNP
Type
0 5 10 15
#Mutations

B

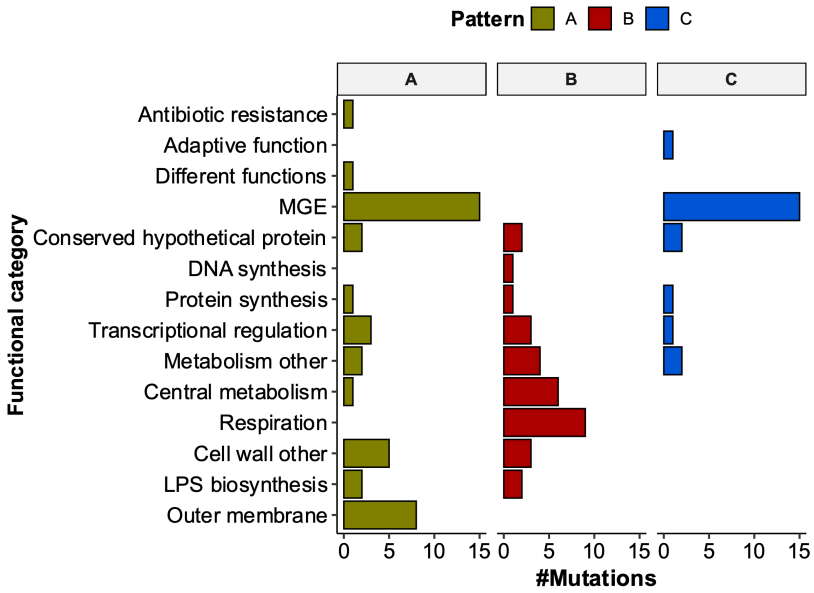
Pattern A B C
A
B
C
Antibiotic resistance
Adaptive function
Different functions
MGE
Conserved hypothetical protein
DNA synthesis
Protein synthesis
Transcriptional regulation
Metabolism other
Central metabolism
Respiration
Cell wall other
LPS biosynthesis
Outer membrane
Functional category
0 5 10 15
#Mutations

Fig.4

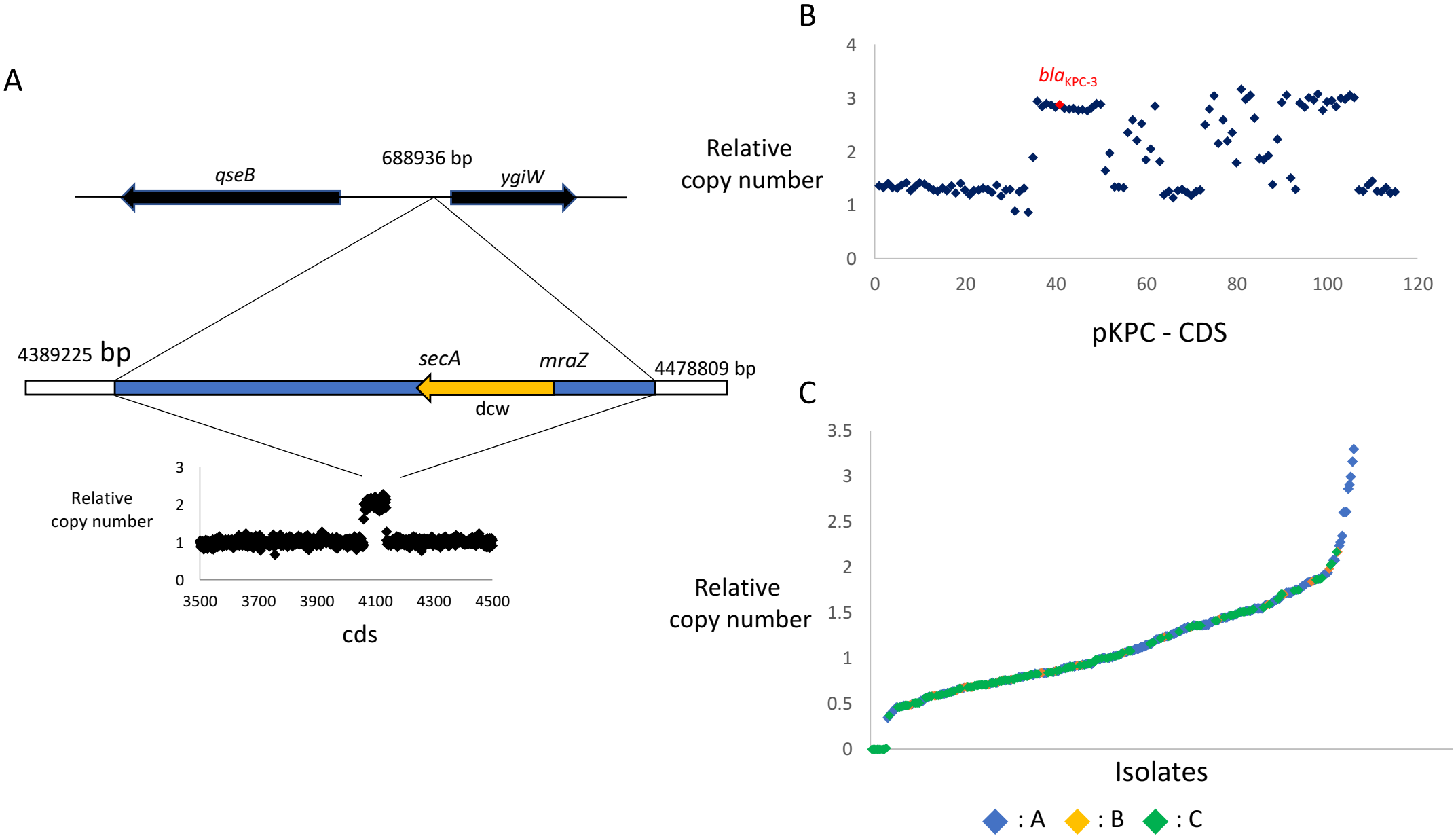
A
688936 bp
qseB
ygiW
4389225 bp
secA
mraZ
4478809 bp
dcw
Relative
copy number
3
2
1
0
3500
3700
3900
4100
4300
4500
cds
B
Relative
copy number
blaKPC-3
4
3
2
1
0
0
20
40
60
80
100
120
pKPC - CDS
C
Relative
copy number
3.5
3
2.5
2
1.5
1
0.5
0
Isolates
: A
: B
: C

Fig.5